

On the Relationship between the North Atlantic Meridional Overturning Circulation and the Surface-Forced Overturning Streamfunction

JEREMY P. GRIST

National Oceanography Centre, Southampton, Southampton, Hampshire, United Kingdom

ROBERT MARSH

National Oceanography Centre, Southampton, and School of Ocean and Earth Science, University of Southampton, Southampton, Hampshire, United Kingdom

SIMON A. JOSEY

National Oceanography Centre, Southampton, Southampton, Hampshire, United Kingdom

(Manuscript received 10 April 2008, in final form 24 February 2009)

ABSTRACT

The influence of surface thermohaline forcing on the variability of the Atlantic meridional overturning circulation (MOC) at mid–high latitudes is investigated using output from three Intergovernmental Panel on Climate Change (IPCC) coupled climate models. The method employed is an extension of the surface-forced streamfunction approach, based on water mass transformation theory, used in an earlier study by Marsh (2000). The maximum value of the MOC at 48°N is found to have a significant lagged relationship with the maximum surface-forced streamfunction in the region north of 48°N with a surface density greater than $\sigma_0 = 27.5 \text{ kg m}^{-3}$. This correlation peaks when the index of the surface-forced streamfunction leads the MOC by 2–4 yr, depending on the coupled model considered. A method for estimating the MOC variability solely from the surface forcing fields is developed and found to be in good agreement with the actual model MOC variability in all three of the models considered when a past averaging window of 10 yr is employed. This method is then applied with NCEP–NCAR reanalysis surface flux fields for the period 1949–2007 to reconstruct MOC strength over 1958–2007. The reconstructed MOC shows considerable multidecadal variability but no discernible trend over the modern observational era.

1. Introduction

Controversy surrounds possible recent decadal to multidecadal changes in the Atlantic meridional overturning circulation (MOC). Estimates from in situ measurements on five occupations over 1957–2004 were used by Bryden et al. (2005) to suggest that the MOC has slowed by $\sim 8 \text{ Sv}$ ($1 \text{ Sv} \equiv 10^6 \text{ m}^3 \text{ s}^{-1}$) since the 1950s, most notably since the early 1990s. However, an alternative approach in which the MOC strength is inferred from the difference in sea surface temperature (SST) between two regions (40°–60°N, 60°–10°W and 40°–60°S,

50°–0°W) has been used to argue that the MOC has actually strengthened by $\sim 3 \text{ Sv}$ since the 1980s (Latif et al. 2006). A third approach, using a 1° ocean model constrained by a range of observations, suggests that the MOC has weakened significantly over 1992–2004 but only by a relatively small amount, $2.47 \pm 0.65 \text{ Sv}$ (Wunsch and Heimbach 2006). Most recently, Cunningham et al. (2007) note that the section estimate of the MOC strength for 2004 used by Bryden et al. (2005) was taken during a period of low overturning relative to the year-long average overturning, and thus they may have overestimated the extent of the MOC weakening.

The variability of the North Atlantic MOC is determined by a combination of buoyancy and wind forcing, with the different roles of these processes being an area of current research (Kuhlbrodt et al. 2007). The buoyancy forcing of the MOC can be attributed to two

Corresponding author address: Dr. Jeremy Grist, Ocean Observing and Climate (256/18), National Oceanography Centre, Southampton, European Way, Southampton, SO14 3ZH, United Kingdom.
E-mail: jeremy.grist@noc.soton.ac.uk

processes: (i) surface fluxes of heat and freshwater and (ii) diapycnal mixing. The latter process comprises a wide range of phenomena, including small-scale diffusive mixing, the breaking of internal waves, entrainment in the vicinity of overflows, and the seasonal cycle of thermocline water entrainment into the surface mixed layer. If the MOC streamfunction is plotted in density space, there is a clear link to water mass transformation due to surface forcing and mixing (Marsh et al. 2000). In spite of the ubiquitous mixing, water mass transformation in the extratropical North Atlantic is dominated by surface density fluxes (Nurser et al. 1999). The implication is that variations in the MOC itself can be largely attributed to changes in the surface fluxes. Subsequently, Marsh (2000) used observation-based monthly datasets of heat and freshwater fluxes, along with surface temperature and salinity fields, to construct the surface-forced streamfunction. His results revealed changes at interannual and decadal time scales, which captured in broad terms the impact on the MOC of substantial changes in Labrador Sea Water (LSW) formation during the period 1980–97.

In this paper, we use output from the control runs of three Intergovernmental Panel on Climate Change (IPCC) models to examine the extent to which estimates of the North Atlantic MOC can be diagnosed from surface fluxes alone. In particular, we extend the method of Marsh (2000) to make use of surface-forced streamfunction estimates at various lags of up to 15 yr to take account of the accumulation over time of the surface forcing signal before it impacts the MOC. Furthermore, we use the relationship between surface buoyancy forcing and the strength of the MOC at 48°N to reconstruct the variability of the MOC at this latitude over the last 50 yr. The attraction over the previous empirical method that Latif et al. (2006) used to reconstruct the MOC is the accommodation of a direct link between thermohaline forcing and the overturning circulation. Our reconstruction of the MOC strength at 48°N is, however, presented in the context that it is limited by errors in the datasets used to estimate thermohaline forcing and the extent to which the overturning circulation is linked in a relatively straightforward way with surface thermohaline forcing (which ignores wind forcing).

2. Methodology, models, and observations

The methodology for determining the surface-forced overturning streamfunction is described in detail in Marsh (2000). Here we present a brief summary of the key points. Averaged over a region of ocean north of latitude θ , the volume flux, $G(\theta, \rho)$, across an isopycnal, ρ , is related to the combined effects of surface density fluxes and mixing. Formally,

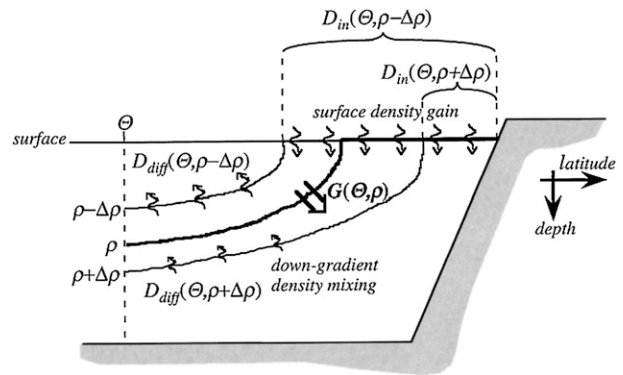


FIG. 1. Schematic diagram of the surface and interior diapycnal density fluxes and the net diapycnal volume flux in a meridional section across an idealized North Atlantic (from Marsh 2000).

$$G(\theta, \rho) = F(\theta, \rho) - \frac{\partial D_{\text{diff}}(\theta, \rho)}{\partial \rho} + C(\theta, \rho), \quad (1)$$

where $F(\theta, \rho)$ is the surface-forced water mass transformation rate across ρ north of θ ; the second term on the right-hand side is the water mass transformation due to diapycnal divergence of the diffusive density flux, $D_{\text{diff}}(\theta, \rho)$; and $C(\theta, \rho)$ is the divergence of the density flux from isopycnal mixing along ρ , also termed cabelling. Under the assumption of fluid incompressibility and a steady state of the water masses, all the water north of θ that is transformed across ρ must be transported southward across θ . Thus, by implication $G(\theta, \rho)$ is the same as the zonally integrated meridional overturning streamfunction or MOC.

From (1) it can be seen that in the absence of mixing, $G(\theta, \rho)$ can be estimated from $F(\theta, \rho)$. Given that water mass transformation in the North Atlantic is predominantly due to surface forcing (Nurser et al. 1999), we have calculated $F(\theta, \rho)$ using output from the control runs of three IPCC models and then examined the extent to which an approximation of $G(\theta, \rho)$ by $F(\theta, \rho)$ corresponds to the MOC from the same control run. Note that $F(\theta, \rho)$ is given by the following formula:

$$F(\theta, \rho) = \frac{\partial D_{\text{in}}(\theta, \rho)}{\partial \rho}, \quad (2)$$

where D_{in} is the area-integrated surface density flux north of wherever the isopycnal ρ outcrops (see schematic in Fig. 1 reproduced from Marsh 2000). We have determined D_{in} from the model surface heat and freshwater fluxes, as well as surface temperature and salinity, using the formula of Schmitt et al. (1989). Values for $F(\theta, \rho)$ were then obtained using Eq. (2) above. Following Marsh

(2000), we take the maximum value of $F(\theta, \rho)$ for $\sigma_0 > 27.45 \text{ kg m}^{-3}$ (where σ_0 is the surface density, $\rho_0 - 1000$) in the region 48°N to 81°N in each model to be a measure of the total surface-forced overturning circulation (SFOC). This maximum value is then compared with the model-derived value of the MOC strength at 48°N .

The model output employed in our study consists of 100-yr sections of the preindustrial control simulations for the following models: the Geophysical Fluid Dynamics Laboratory climate model, version 2.1 (GFDL2.1), the third climate configuration of the Met Office Unified Model (HadCM3), and the Bjerknes Centre for Climate Research model, version 2.0 (BCM2.0). The GFDL2.1 and HadCM3 have z -coordinate oceans, with horizontal resolutions of 1° and 1.25° respectively in the North Atlantic. BCM2.0 has a horizontal resolution of approximately 1.5° in the North Atlantic and is one of a small number of IPCC models run with isopycnic vertical coordinates in the ocean interior. Further details on the formulation of the models can be found in Delworth et al. (2006), Gordon et al. (2000), and Furevik et al. (2003).

Following on from the model analysis, we have obtained observational estimates of the surface-forced streamfunction and, as described later, the Atlantic MOC for the period 1958–2007 (see section 3e). For this part of our study, we have employed monthly-mean sea surface temperature and surface heat and freshwater flux fields from the 40-yr National Centers for Environmental Prediction (NCEP)–National Center for Atmospheric Research (NCAR) Reanalysis (Kalnay et al. 1996), extended up to 2007, and sea surface salinity from Boyer et al. (2005). The salinity dataset consists of annual fields determined from pentadal averages for 1955–59 to 1994–98. For the years before the start and after the end of the salinity dataset, the climatology was used.

3. Results

a. North Atlantic MOC and surface-forced overturning circulation in the models

The mean North Atlantic MOC for each of the models is plotted in Figs. 2a–c; positive values indicate clockwise overturning. Time series of the MOC strength at 48°N for each model are plotted in Fig. 2d. This latitude has been chosen for its proximity to main regions of North Atlantic deep water formation. The mean (and standard deviation) MOC strength is $21.9(\pm 1.4)$ Sv in GFDL2.1, $17.7(\pm 1.0)$ Sv in HadCM3, and $14.5(\pm 1.1)$ Sv in BCM2.0. In addition to the difference in MOC strength, BCM2.0 exhibits some differences typical for an isopycnal model; in particular, the abyssal cell associated with Antarctic Bottom Water is absent and the return flow occurs at

greater depth. We also note that there is greater overturning in HadCM3 compared to BCM2.0 north of 65°N . The stronger HadCM3 overturning is partially due to a deepened Greenland–Iceland–Scotland Ridge (Roberts and Wood 1997). Note that the GFDL2.1 model output does not include values of the overturning streamfunction north of 65°N and so in this region we cannot compare it with the other models. By using these three models, which span the typical range of MOC strengths found in the IPCC evaluation (e.g., Gregory et al. 2005) and have different architectures, we are able to investigate the relationship between the MOC and the surface-forced overturning across a range of conditions.

The mean surface-forced meridional streamfunction for each of the models, derived using the methodology outlined in section 2, is shown in Figs. 3a–c. In overall terms, the three models have a similar appearance, with progression of northward flow toward higher density with increasing latitude. Larger differences are apparent in the horizontal streamlines, which correspond to southward interior flow. The degree to which these streamlines are bunched together varies between the models, indicating the extent of surface homogenization in density (i.e., the extent to which water mass formation is centered on a narrow range of density). In HadCM3, the streamlines are most spaced out (compared to GFDL2.1 and BCM2.0), indicating that surface water mass formation is occurring more evenly across a wide density range. This may be due to more restricted overturning at higher latitudes in GFDL2.1 (compared to HadCM3) and the isopycnal formulation of BCM2.0, which can restrict the extent of diapycnal mixing.

b. Model insights into the relationship between total MOC and the SFOC index

Marsh (2000) considered the extent to which the surface forced overturning circulation can be used to estimate the total MOC. He noted that the effects of surface forcing must dominate diapycnal mixing in order for useful estimates to be obtained, and this is expected to be the case for the North Atlantic region considered in the present study. We now examine the strength of the relationship between the SFOC index and the maximum value of the total MOC using values derived from the three coupled climate models described in section 2. One of our goals here is to examine, for the first time, whether there is any lagged dependence in the relationship between the two indices. Based on the time it takes for an oceanic signal of a heat flux anomaly in the Nordic Seas to reach 50°N (Grist et al. 2007, 2008), it may be worth considering the integrated effects of surface forcing over as much as the previous 10 yr. A somewhat shorter

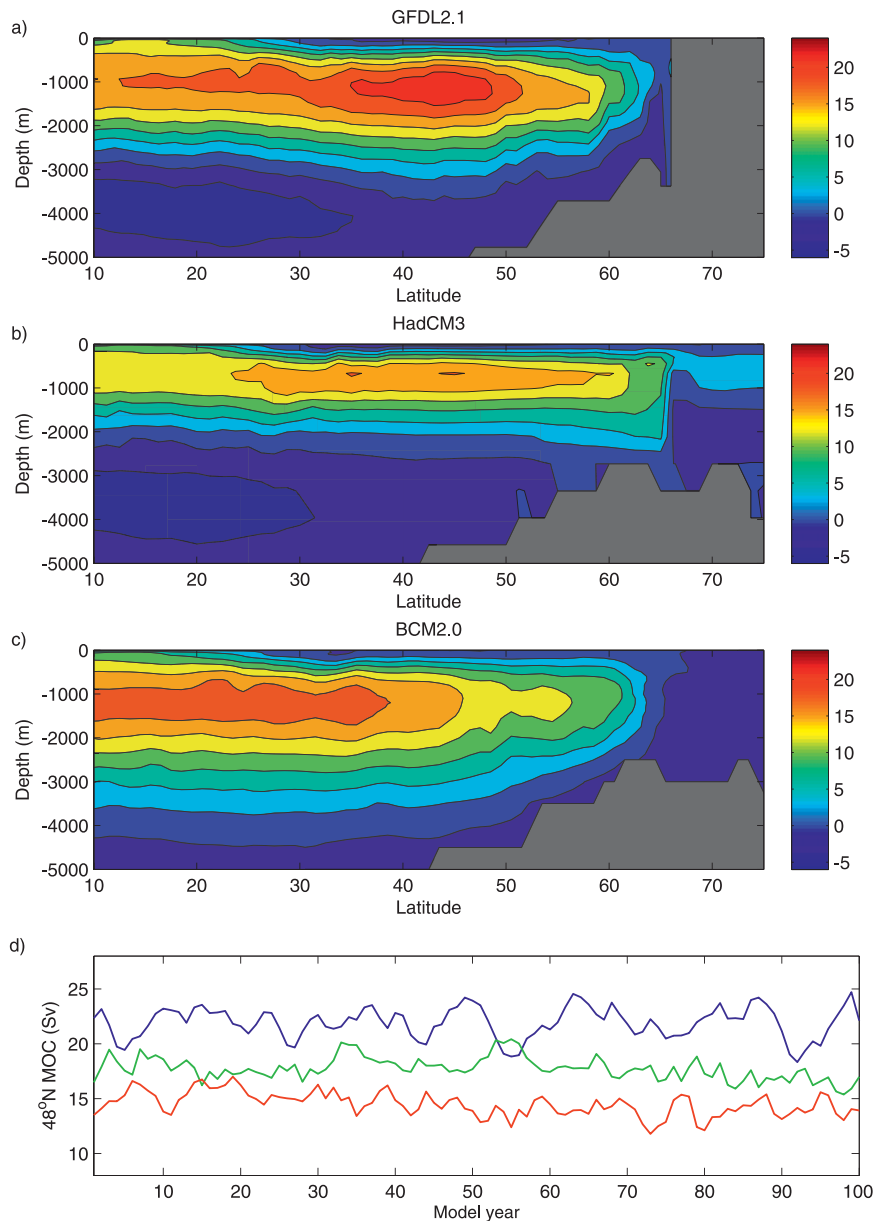


FIG. 2. (a)–(c) Mean Atlantic meridional overturning streamfunction (Sv) from 100 yr of the control run of (a) GFDL2.1, (b) HadCM3, and (c) BCM2.0. (d) Corresponding 100-yr time series of the maximum MOC at 48°N for GFDL2.1 (blue line), HadCM3 (green line), and BCM2.0 (red line).

adjustment time scale is suggested by both theory and results obtained with a reduced-gravity shallow water model of the upper branch flow, in which a thermohaline overturning of 10 Sv is instantaneously “switched on” at 60°N (Johnson and Marshall 2002). More complete general circulation models forced with realistic surface fluxes indicate that there is a more delayed baroclinic response of the ocean circulation to characteristic atmospheric variability; for example, Eden and Willebrand

(2001) find a 6–8-yr lagged response of the overturning at 48°N to the North Atlantic Oscillation (NAO) (enhanced overturning follows a switch to positive NAO conditions). We note that this possibility was not considered by Marsh (2000). If a lagged relationship can be established using the model output, it may enable (i) more accurate historical estimates of the MOC to be obtained from observed surface forcing fields and (ii) the potential to obtain near-term (up to about 5 yr) predictions of MOC variability.

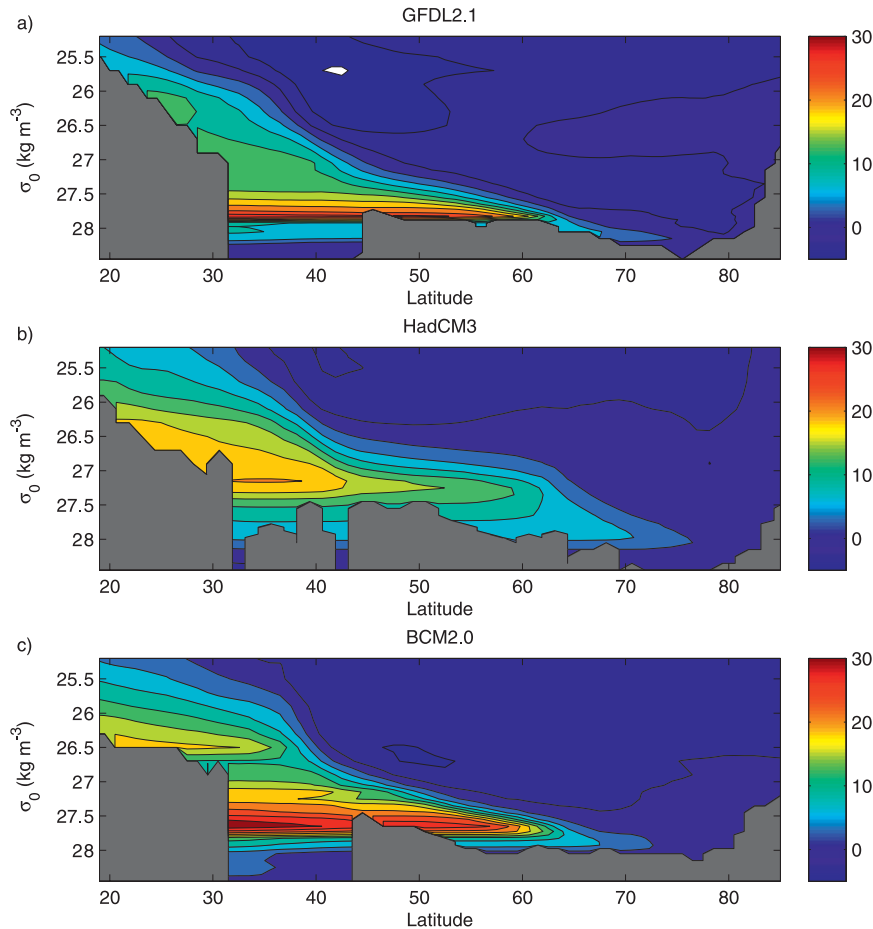


FIG. 3. Mean Atlantic surface-forced overturning streamfunction (Sv) calculated using 100 yr of surface flux data from the control runs of (a) GFDL2.1, (b) HadCM3, and (c) BCM2.0. A mask is applied to σ_0 values greater than the maximum σ_0 at that latitude band.

Time series of the SFOC index for each of the three models are shown in Fig. 4 together with the MOC series shown previously in Fig. 2d for comparison; the mean and standard deviation of the SFOC values for each model are given in Table 1. In all three models, the SFOC time series show strong variability (standard deviations in the range 2.8–5.2 Sv) at interannual time scales that is not present in the MOC. This is to be expected given the stronger influence of short-time scale atmospheric processes on the SFOC index. Note that we will show in section 3c that much better agreement with the MOC variability is obtained when the SFOC is averaged over a 10-yr interval.

Differences between the total MOC and SFOC mean values are model dependent. In HadCM3, the total MOC mean value exceeds the SFOC mean value by ~ 4 Sv. This implies that processes additional to buoyancy forcing act to increase the southward flow (and hence the MOC). Indeed, Gordon et al. (2000) explain

that HadCM3 has a modified convective adjustment in the region of the Denmark Straits and Iceland–Scotland Ridge to better represent the downslope mixing of the overflow water. In the other two models, the SFOC is considerably stronger than the MOC, by ~ 7 Sv (GFDL2.1) and ~ 15 Sv (BCM2.0). The more intense SFOC in these models must be offset by substantially stronger diapycnal mixing in GFDL2.1 and BCM2.0. This may seem surprising because BCM2.0 features an isopycnal-coordinate ocean, free of the spurious diapycnal mixing that is often substantial (and a somewhat elusive component of total diapycnal mixing) in models with level-coordinate oceans (such as GFDL2.1 and HadCM3). However, at high latitudes, most of the diapycnal mixing in isopycnal-coordinate ocean models is actually accomplished through horizontal mixing in the mixed layer and mixed layer entrainment (Nurser et al. 1999). Although investigation of the respective diapycnal budgets is beyond the scope of this paper, we

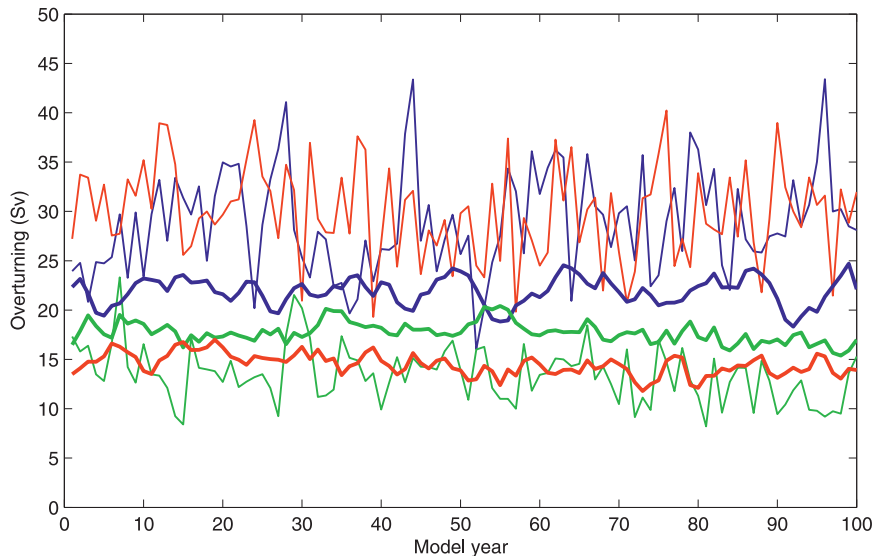


FIG. 4. Time series of the maximum MOC (Sv) at 48°N (thick lines) and the maximum surface-forced overturning streamfunction (Sv) in the domain $48^{\circ}\text{--}81^{\circ}\text{N}$, $\sigma_0 > 27.5$ (thin lines) (termed SFOC in the main text) for GFDL2.1 (blue), HadCM3 (green), and BCM2.0 (red).

note that each model features a distinct vertical mixing scheme. Vertical diffusivity in HadCM3 varies continuously with depth, from a minimum of $0.103\text{ cm}^2\text{ s}^{-1}$ at the surface to $1.468\text{ cm}^2\text{ s}^{-1}$ at the bottom (Table A in Gordon et al. 2000). GFDL2.1 uses a vertical diffusivity of $0.3\text{ cm}^2\text{ s}^{-1}$ in the pycnocline poleward of 40°N and a value of $1.2\text{ cm}^2\text{ s}^{-1}$ in the deep ocean (Gnanadesikan et al. 2006). Although not specified in Furevik et al. (2003), diapycnal diffusivity in MICOM (the ocean component of BCM2.0) varies inversely with local stratification and can reach high values in the weakly stratified high latitudes.

Correlation coefficients between the SFOC index for each model and the corresponding total MOC strength at 48°N have been determined for lead/lag intervals up to 10 yr; the results are shown in Fig. 5. Using the method of Bretherton et al. [1999, their Eq. (31)], the number of effective degrees of freedom was calculated by an analysis of the autocorrelation function of both the SFOC and the MOC time series. The value of the 95% significance level is slightly different for each model, so we have only plotted the mean value of the three (0.25) as a reference. A robust result across the models is that MOC intensity is significantly correlated with the SFOC index when the surface forcing leads by a few years. In HadCM3, the correlation coefficient reaches 0.46 when surface forcing leads the MOC by 4 yr, whereas in GFDL2.1 the maximum correlation value of 0.39 occurs at a lead time of 3 yr. The BCM2.0 model has a peak value of 0.34 at a shorter lead time of 2 yr. Note that in BCM2.0 there is also a significant correlation (0.29)

when the MOC leads the surface forcing by 5 yr; this feature may reflect a delayed influence of variations in the northward transport of warm water by the MOC on the surface forcing at high latitudes through modification of the sea–air temperature difference. However, because it is not evident in the two other models considered we do not consider it further here.

c. Estimates of the MOC based on past averaging of the SFOC index

The main result of the analysis above is that all three models show the MOC is positively correlated with the SFOC index in the preceding decade. This suggests that by averaging the SFOC index over a number of years prior to that being considered (referred to hereafter as *past averaging*), useful estimates of the MOC variability may be obtained. We now explore this possibility using the MOC and SFOC time series for each of the models considered previously. For this part of the analysis, the 100-yr mean values of the MOC and SFOC are first subtracted from the output for each model to obtain time series of the MOC and SFOC anomalies; this allows

TABLE 1. Mean and standard deviation (Sv) of the MOC and SFOC index values for the three models considered.

Model	MOC (mean)	SFOC (mean)	MOC (std dev)	SFOC (std dev)
GFDL2.1	21.9	28.8	1.4	5.2
HadCM3	17.7	13.5	1.0	2.8
BCM2.0	14.5	29.9	1.1	4.7

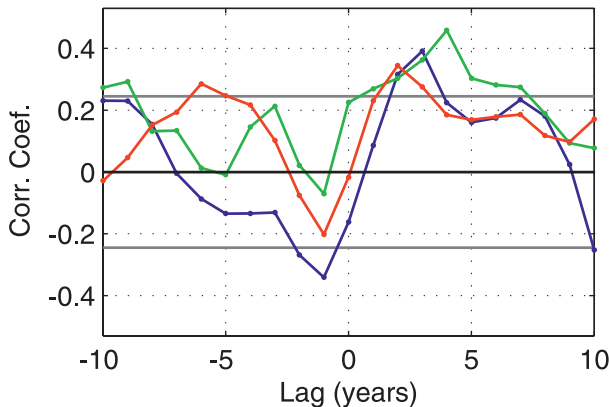


FIG. 5. Variation of the correlation coefficient between the maximum MOC at 48°N and the SFOC index with time lag, for lag intervals of -10 to $+10$ yr, for GFDL2.1 (blue), HadCM3 (green), and BCM2.0 (red). Positive lags indicate the SFOC index leading the MOC. The gray horizontal lines indicate the mean 95% significance level for the three models. The effective number of degrees of freedom for each model are 60 (GFDL2.1), 74 (HadCM3), and 67 (BCM2.0), as calculated by the method of Bretherton et al. (1999).

a clearer comparison to be made between the variability in the MOC and SFOC indices.

Past averaged values of the SFOC anomaly index for time intervals of 3, 6, 10, and 15 yr have been obtained and compared with the MOC anomaly index for each model. The results of this comparison are shown in Figs. 6 and 7 with corresponding statistical measures in Tables 2 and 3. A general trend toward smaller-amplitude SFOC index variability is observed as the past averaging period increases. At 3-yr and 6-yr time scales, the variability of the SFOC anomaly index (as measured, for example, by standard deviation values of 1.9 and 1.5 Sv respectively for HadCM3) is stronger than the corresponding MOC variability value (1.0 Sv). However, for a past averaging interval of 10 yr the level of variability of the SFOC anomaly index is close to that for the MOC, and there is an encouraging level of agreement between the time series. With the exception of the first half of the GFDL2.1 time series, the correlation between the indices in the three models is significant at the 95% level [using the method of Bretherton et al. (1999)]. The agreement is particularly evident for HadCM3 (standard deviation of SFOC = 1.2 Sv; MOC–SFOC correlation coefficient $r = 0.64$), for which the MOC peak between model years 30 and 40 is reproduced by the SFOC anomaly index, as is the downward trend from years 70 to 100. For the other two models, the level of agreement is less striking but still encouraging for the 10-yr past averaging interval. For GFDL2.1, a close correspondence between the SFOC and MOC anomalies is observed in the second half of the period considered ($r = 0.70$ for

years 50–100, compared with $r = 0.36$ for the full 100-yr period). For BCM2.0, the slow decline of the MOC from about years 20 to 60 is reproduced by the SFOC index, as is the slight upward trend thereafter, although the correspondence between individual events is less clear cut ($r = 0.57$ for the full period). For a past averaging interval of 15 yr, the agreement between the SFOC and MOC is poorer than at 10 yr, indicating that for this long an interval, relevant information is being lost.

In summary, useful estimates of both the timing and amplitude of variability in the MOC can be obtained by past averaging the SFOC index over the previous 10 yr, with the best results being obtained for HadCM3. In the latter case, 41% of the variance in the MOC time series can be explained using the SFOC index (i.e., from surface forcing data alone).

d. The observation-based surface-forced meridional streamfunction

We now shift the focus of our study from model-based results to the observational record. In this subsection, we discuss the main characteristics of the long-term mean surface-forced meridional streamfunction as determined from observations. We then carry out a reconstruction (in section 3f) of MOC variability over the last 50 yr using the past averaging method developed above.

The annual-mean surface-forced meridional streamfunction, derived from the NCEP–NCAR reanalysis and Boyer et al. (2005) observational fields, for the North Atlantic is shown in Fig. 8a. The positive values that dominate Fig. 8a are indicative of clockwise overturning. The large-scale pattern is of the northward flow weakening at progressively higher σ_0 as fractions of the flow return southward in branches. In addition, there are regional cells of overturning restricted to specific ranges of σ_0 and latitude. As previously described by Marsh (2000), these regional features are associated with regions of water mass formation well known from hydrography. In particular, the two main areas of dense water formation at mid–high latitudes are (i) 65° – 81°N , $\sigma_0 > 27.82 \text{ kg m}^{-3}$ where ~ 9 Sv of Greenland Sea Deep Water (GSDW) is formed, and (ii) 48° – 65°N , $27.6 \text{ kg m}^{-3} < \sigma_0 < 27.75 \text{ kg m}^{-3}$, where ~ 14 Sv of LSW is formed. To capture the influence of both LSW and GSDW formation, we again use the SFOC index introduced in section 2, which was defined to be the maximum value of the surface-forced overturning circulation for $\sigma_0 > 27.45 \text{ kg m}^{-3}$ in the region 48° – 81°N . The regions of $\sigma_0 - \theta$ used to define LSW, GSDW, and the SFOC index are indicated on Fig. 8a.

Time series of the SFOC index as well as the formation of LSW and GSDW, determined using the density ranges specified above, are shown in Fig. 8b. Ideally both

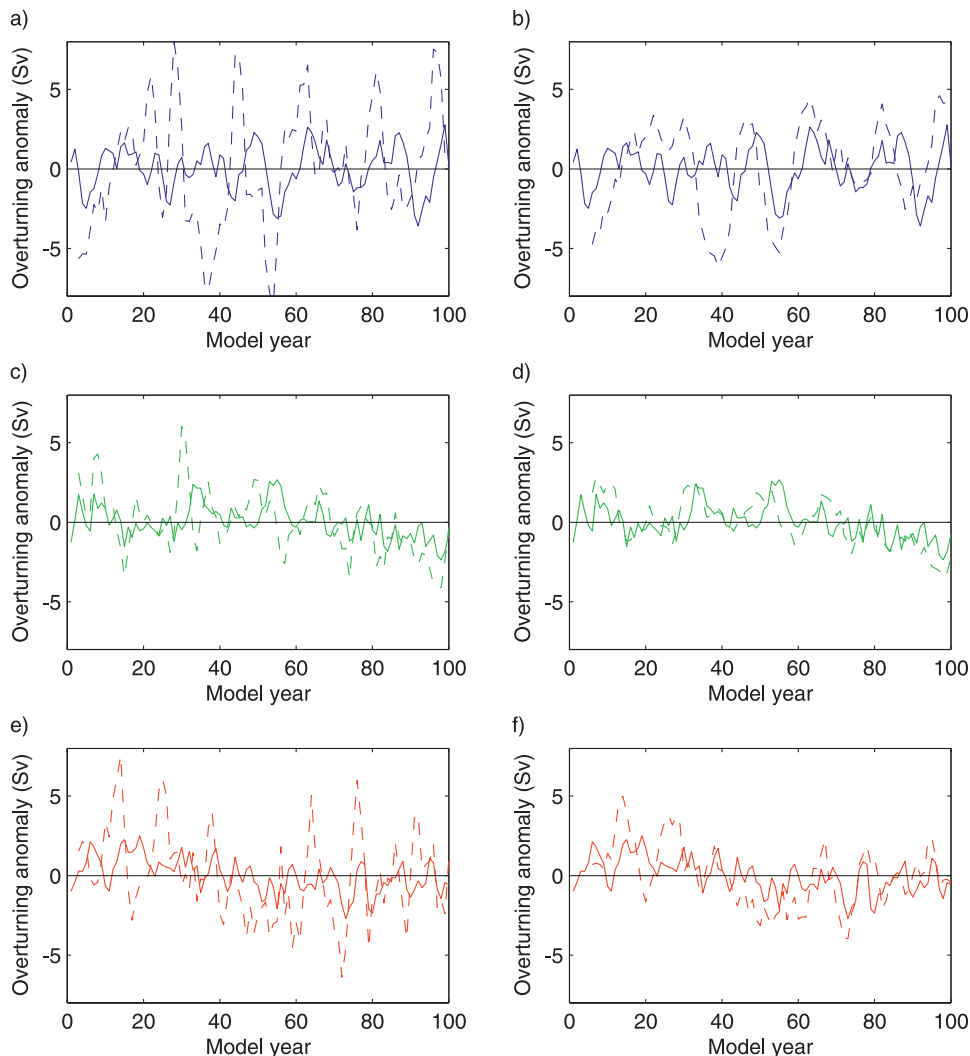


FIG. 6. (a),(c),(e) Time series of the anomaly in the maximum MOC at 48°N (solid lines) and the past averaged SFOC index (dashed lines) for (a) GFDL2.1, (c) HadCM3, and (e) BCM2.0, where the past averaging interval is 3 yr (the current year and the previous 2 yr). (b),(d),(f) As in (a),(c),(e), respectively, but for a past averaging interval of 6 yr.

LSW and GSDW time series in Fig. 8b would be evaluated with independent hydrographic estimates of water formation rates. This is made difficult, first, because of the scarcity of continuous observations of the ocean interior and second, because where observations do exist, they need to be considered with the caveat that convection can be a very localized phenomena, making it difficult to distinguish between lateral variability and changes in time (Ronski and Budéus 2005). Nonetheless, it is important where possible to consider the available observations because they offer a means to validate the surface forced overturning diagnostic used in this study.

The time series of LSW indicates that there have been three periods of enhanced LSW formation: 1961–63,

1979–81, and 1990–97. The mean formation rates during these periods were 15.8, 18.3, and 16.7 Sv compared to the series-long mean of 12.1 Sv. An observational time series of LSW thickness compiled by Curry et al. (1998) confirms an increase in LSW in the early 1960s and from 1990 to 1995. Curry et al. (1998) do not show the increase during 1979–81, although an examination of the long running time series of temperature and salinity profiles in the central Labrador Sea (e.g., Haine et al. 2007; Yashayaev et al. 2003) suggests that the region was convectively active at some point between 1976 and 1983. The GSDW transformation rate, shown by the dashed line in Fig. 8b, has a mean value of 7.9 Sv. The time series exhibits considerable interannual variability,

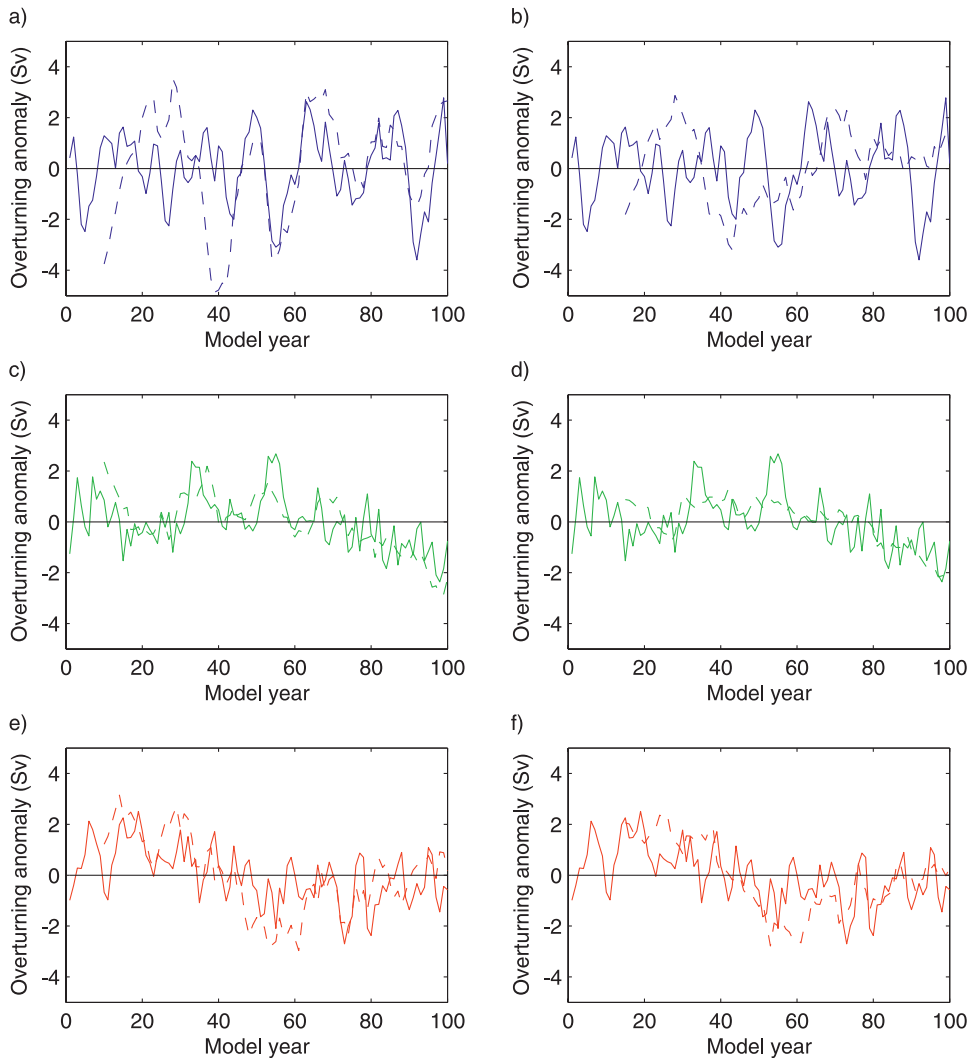


FIG. 7. (a),(c),(e) Time series of the anomaly in the maximum MOC at 48°N (solid lines) and the past averaged SFOC index (dashed lines) for (a) GFDL2.1, (c) HadCM3 and (e) BCM2.0, where the past averaging interval is 10 yr (the current year and the previous 9 yr). (b),(d),(f) As in (a),(c),(e), respectively, but for a past averaging interval of 15 yr.

but its longer-term variability is characterized by water mass formation rates that were elevated to a mean of 8.8 Sv from 1949 to 1985 and, apart from a spell between 1995 and 1997, have remained relatively diminished since (with a mean of 6.4 Sv). There is no continuous

hydrographic record against which this can be validated. However, reviewing the available hydrographic and meteorological evidence, Dickson et al. (1996) concluded that for the late 1950s through the early 1970s there was enhanced Greenland Sea convection, after

TABLE 2. Values for the correlation coefficient (*r*) between the MOC anomaly index and the past averaged value of the SFOC anomaly index for various past averaging intervals.

Model	Past averaging interval (yr)			
	3	6	10	15
GFDL2.1	0.12	0.28	0.36	0.02
HadCM3	0.40	0.62	0.64	0.59
BCM2.0	0.32	0.48	0.57	0.58

TABLE 3. Standard deviation (Sv) of the SFOC anomaly index for various past averaging intervals.

Model	Past averaging interval (yr)			
	3	6	10	15
GFDL2.1	3.8	2.9	2.1	1.4
HadCM3	1.9	1.5	1.2	0.9
BCM2.0	2.8	2.0	1.5	1.4

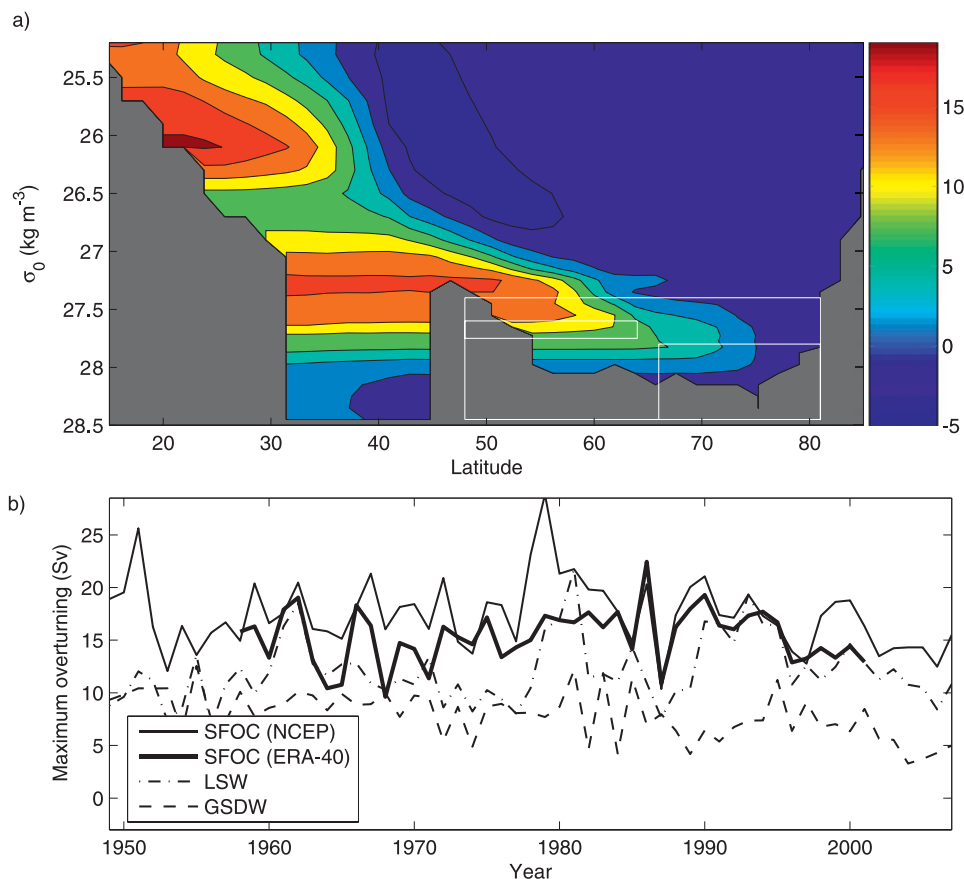


FIG. 8. (a) Annual-mean surface forced overturning streamfunction (Sv) as a function of σ_0 , determined from the NCEP–NCAR Reanalysis. A mask is applied to σ_0 values greater than the maximum σ_0 at that latitude band. (b) Time series of the maximum surface-forced overturning streamfunction in the domains 48° – 81° N, $\sigma_0 > 27.5$ or SFOC (NCEP, thin solid line; ERA-40, thick solid line); 48° – 64° N for $27.65 < \sigma_0 < 27.725$ or LSW (dotted–dashed line, NCEP only); and 66° – 81° N, $\sigma_0 > 27.82$ or GSDW (dashed line, NCEP only). The corresponding regions of $\theta - \sigma_0$ space are indicated by the white boxes in (a).

which it diminished and generally remained at a reduced state. Also consistent with our GSDW time series is the work of Rhein (1996), who reported that CFC profiles in the Greenland Sea indicated that “deep convection rates remained small between 1989–93.” Although there is considerable interannual variability in the SFOC time series (mean value of 17.4 Sv), it is also strongly modulated by interdecadal variability. After a strong SFOC of ~ 26 Sv in 1951, the circulation weakened during the 1950s and then returned to around average in the 1960s and early 1970s. Between 1978 and 1983 the SFOC was anomalously strong, with a mean of 22.4 Sv. Since that period, with the exception of a spell from 1988 to 1991, the SFOC has generally been of weaker strength.

We note there are observational limitations on the calculation of the surface-forced streamfunction. As discussed by Wunsch (2005), the uncertainty of NCEP

fluxes over the ocean is not routinely documented or easily inferred. The observational uncertainty in the SFOC index will be no smaller than the difference between the estimates produced by the NCEP reanalysis and the European Centre for Medium-Range Weather Forecasts (ECMWF) reanalysis. To this end, the calculation of the SFOC index from ECMWF is shown alongside that from NCEP in Fig. 8b. With the exception of the years 1978–80, when the NCEP version of SFOC is considerably larger, the interannual variability of SFOC is very similar between the NCEP and ECMWF versions. In the near future an update of the National Oceanography Centre, Southampton (NOCS) air–sea flux climatology (Berry and Kent 2009) will include flux uncertainty estimates. This will enable an estimate of the SFOC with error ranges to be determined, which will provide a useful point of reference for the reanalysis-based estimates.

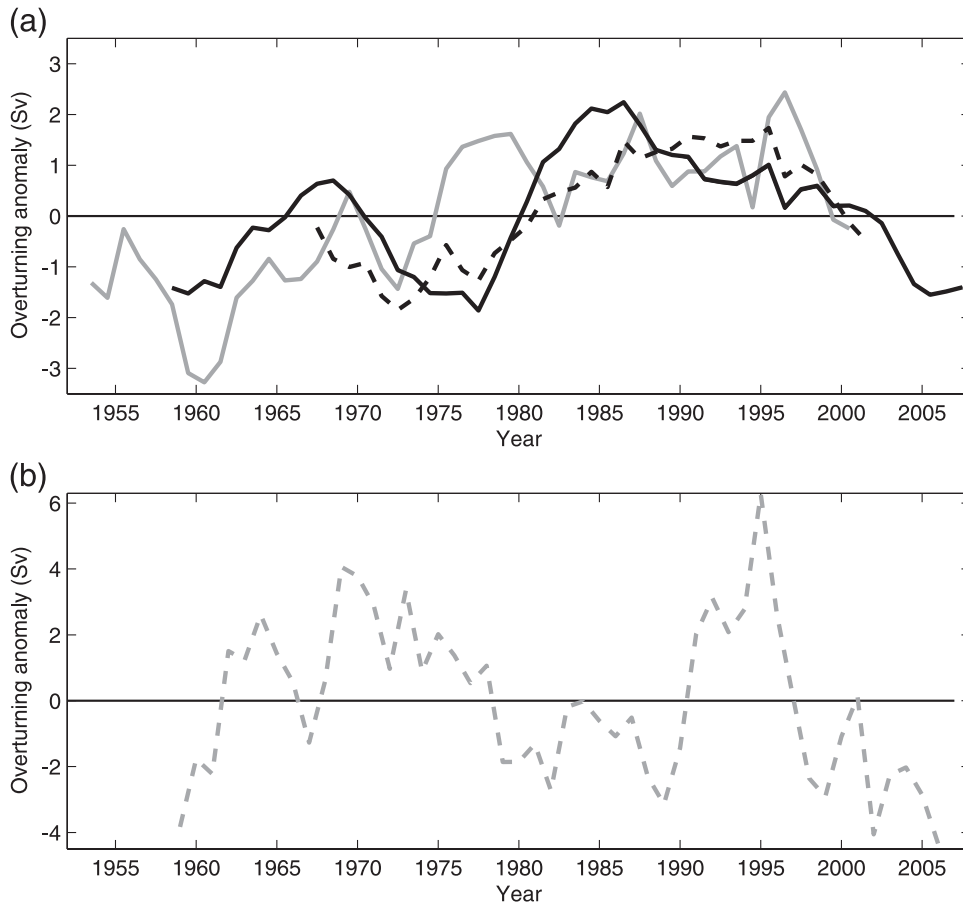


FIG. 9. (a) Reconstruction of the maximum MOC (Sv) at 48°N for 1958–2007 using the past averaged SFOC index with a 10-yr averaging interval, as determined from the NCEP–NCAR Reanalysis (solid black line) and for 1962–2001, from the ERA-40 analysis (dashed black line). Also shown is the GECCO estimate of the maximum MOC at 48°N, 1952–2001 (solid gray line). (b) Reconstruction of the maximum MOC at 50°N, for 1959–2006, from Balmaseda et al. (2007; dashed gray line). In both panels the values are shown as departures from the mean of the respective time series.

e. Reconstruction of the MOC variability for 1958–2007

The past averaging method developed in section 3b, with a 10-yr averaging interval, is now used with SFOC index values obtained from the NCEP–NCAR surface-forcing fields to produce an observation-based estimate of the variability in the MOC strength at 48°N for 1958–2007 (Fig. 9a). We again show the reconstruction as a departure from the mean. The reconstruction suggests that the MOC was about 1.5 Sv weaker than the mean at the start of the 1960s. It then increased to close to the mean magnitude at the end of the 1960s. There followed a period of decline to the weakest level in the reconstruction in 1977. After 1977, there is an abrupt transition to a stronger state and by the mid-1980s the overturning strength is some 2 Sv greater than the longer-term mean. The overturning in the reconstruction was stronger than

normal between 1980 and 2001. However, after the mid-1980s there was a steady decrease toward a weaker state, from which there has been a slight recovery in the last year. A characteristic similar to that in other reconstructions (Latif et al. 2006; Köhl and Stammer 2007) is that MOC variability over the last 50 yr is dominated by interdecadal variability as opposed to any obvious long-term trend.

As part of the German contribution to the Estimating the Circulation and Climate of the Ocean Project (GECCO), Köhl and Stammer (2007) produced a dynamically consistent estimate of the Global Ocean with an integration of the ECCO–Massachusetts Institute of Technology (MIT) ocean model from 1952 to 2001. Their time series of the maximum MOC strength at 48°N is also shown in Fig. 9 and is seen to be in good agreement with the reconstruction that we have obtained from the surface fields alone without a model. The ocean

model was forced with NCEP fluxes, so their MOC time series is not completely independent of ours. However, importantly, the ocean model was additionally constrained with the assimilation of most available in situ ocean and surface observations since 1950, as well as more recent satellite observations. Thus, the comparison of the GECCO time series with the current reconstruction in Fig. 9 is of interest. There are differences between the two time series; notably, their anomalies are of opposite sign between 1975 and 1980. Nonetheless, there are considerable similarities in the reconstructions, including the anomalously weak MOC in the early 1960s, with a smaller short-lived peak toward the end of the decade, and the positive anomaly after 1980, which was maintained until it moved to a negative phase around 2000. These results suggest that the SFOC technique is capable of producing similar estimates of MOC variability to those obtained through state-of-the-art data assimilation.

An historical reconstruction of the ocean state using an approach similar to the GECCO group has been undertaken by Balmaseda et al. (2007). They assimilated in situ observations into an integration of the HOPE ocean model (Wolff et al. 1997) from 1959 to 2006. The Balmaseda et al. (2007) estimate of the ocean state differs from that of Köhl and Stammer (2007) in two significant ways. First, Balmaseda et al. (2007) forced the ocean with 40-yr ECMWF Re-Analysis (ERA-40), as opposed to NCEP, surface fluxes; second, they used a different assimilation scheme. The reconstruction of the MOC at 50°N from Balmaseda et al. (2007) is shown in Fig. 9b. We note that differences between our MOC reconstruction at 48°N and 50°N are negligible (not shown). Although the Balmaseda et al. (2007) reconstruction shows the MOC decline since the mid-1990s seen in both our NCEP and ERA-40 reconstructions, for most of the time series the temporal evolution is different. The implication is that the lack of consensus between the two ocean reanalyses is probably due to differences in the assimilation techniques rather than differences in the two atmospheric reanalysis products that are used to force the ocean and that also form the basis of our reconstructions in Fig. 9.

Latif et al. (2006) suggested that the difference in SST between two regions in the North and South Atlantic (40°–60°N, 60°–10°W and 40°–60°S, 50°–0°W) could be used to infer the strength of the MOC at 30°N. The evolution of the MOC strength at 48°N obtained using our method is different from that of the index in Fig. 2 of Latif et al. (2006), with the anomalies often being of opposite sign. Agreement between our reconstructions at 48°N and others (e.g., Latif et al. 2006; Knight et al. 2005) at 30°N is not expected because model results in-

dicate that MOC variability is not coherent between these latitudes (Bingham et al. 2007). However, it is noteworthy that Marsh (2000) concluded that north of 15°N, the relatively minor role played by mixing may allow the MOC to be estimated from the surface-forced overturning. Therefore, in future work we intend to examine if the technique used here can be profitably extended to the subtropical latitudes in order to reconstruct variability at a latitude comparable to Latif et al. (2006). In this context, we note that Wunsch and Heimbach (2006) estimated the strength of the MOC at 26°N by constraining a 1° ocean model with a large number of surface and subsurface observations from 1992 to 2004. They found a weak but statistically significant decline of 2.47 ± 0.65 Sv in MOC strength during this period.

4. Summary and discussion

We have investigated the role of surface thermohaline forcing in the variability of the Atlantic MOC at mid-high latitudes using output from three IPCC coupled climate models. The method that we have employed is based on the surface-forced streamfunction approach used in an earlier study by Marsh (2000), extended to consider longer time periods for the effects of the high-latitude surface forcing to impact the circulation. Our focus has been on variability at 48°N because it lies relatively close to the major deep water formation regions of the Nordic and Labrador Seas; variability at this latitude has also been the subject of recent ocean synthesis studies (Köhl and Stammer 2007; Balmaseda et al. 2007).

The maximum value of the MOC at 48°N is found to have a significant lagged relationship with the maximum surface-forced streamfunction over subpolar latitudes from the preceding years. This correlation peaks between 2 and 4 years earlier depending on the coupled model considered. Estimates of the MOC variability were then determined solely from the surface-forced streamfunction averaged over various time intervals prior to the time being considered (referred to as the past averaging method). Good agreement with the actual model MOC variability in all three of the models considered was obtained with a past averaging period of 10 yr. Shorter intervals led to MOC variability estimates which were of greater amplitude than those obtained directly from the model, whereas longer intervals produced too weak a reconstruction of the MOC variability.

Using historical observations of surface density fluxes, the surface-forced streamfunction was calculated for the period 1949–2007. By using the 10-yr past averaging technique, the observational estimate of the SFOC index was then used to reconstruct the MOC variability at

48°N for 1958–2007. Our results support other assertions that the MOC varies appreciably (anomalies of 1.5–3 Sv) at multidecadal time scales (Latif et al. 2006). The MOC reconstruction does not exhibit any obvious long-term trend such as that originally reported at 26°N by Bryden et al. (2005).

Our reconstruction of MOC variability at 48°N compared well with the reconstruction at the same latitude from GECCO (Köhl and Stammer 2007). The GECCO results were derived from an ocean model, forced with NCEP fluxes, and constrained with the assimilation of most of the available ocean subsurface, surface, and satellite observations since 1950. The similarity of the two reconstructions suggests that the SFOC technique is capable of producing estimates of MOC variability similar to those obtained through state-of-the-art data assimilation.

The similarity of our reconstruction to that of GECCO is not affected much if the SFOC is derived from ERA-40 surface fluxes instead of NCEP fluxes. However, the ocean reanalysis of Balmaseda et al. (2007), which is forced with ERA-40 fluxes, corresponds little either to our reconstructions or to that from the GECCO group. The implication is that the uncertainties between the different flux datasets we used in our reconstruction are probably not the cause of differences between the MOC reconstructions from different ocean reanalyses.

We have discussed extending our analysis to subtropical latitudes in subsequent work (Josey et al. 2009). However, we note here that model hindcasts reveal that the MOC south of ~40°N is dominated by interannual variability, whereas decadal variability is much clearer to the north of this latitude (Bingham et al. 2007). Hence, we anticipate a weaker relationship between mid–high latitude surface forcing and variability of the MOC in the subtropics. A key point of reference for such a study is the Rapid Climate Change Programme (Rapid) observing array, which became operational in 2004 and will in time provide a valuable multiyear description of the temporal evolution of the MOC at 26°N (Cunningham et al. 2007). We note that our reconstruction suggests that Rapid monitoring began at a time in the reanalysis era in which the MOC at 48°N was relatively weak. This serves as a reminder that an observed increase in the MOC over the first few years of the array deployment would be entirely consistent with the type of interdecadal variability seen in Fig. 9.

The coverage of surface observations for the North Atlantic has historically been more comprehensive than at depth, and this is likely to remain the case. Consequently, it is of significant interest to see if the MOC strength can be diagnosed from the surface density fluxes. Despite similarities between our reconstruction and that

from GECCO, an important proviso from this study is that based on the IPCC models used here, the ability of the surface density forcing to explain the variability of the MOC is at most 41%. This might be improved if we were able to account for the mixing in Eq. (1). In addition to thermohaline forcing, variations in wind forcing (such as those related to the North Atlantic Oscillation) may alter horizontal transports, with implications for the MOC. There may be further nonlinear connections between surface density fluxes and sinking rates that are linked to variations in stratification, unaccounted for by local surface density fluxes. Such variability may be controlled by a combination of advection and mixing, such as that associated with the Great Salinity Anomaly (Dickson et al. 1988). A significant proportion of the MOC variability in the models may therefore be in response to anomalies in wind forcing and high-latitude freshwater transports.

To conclude, we have shown that a method based on past averaging of the surface-forced overturning streamfunction is capable of producing useful estimates of interdecadal variability of the MOC at mid–high latitudes as represented by 48°N. Thus, it has the potential to identify long-term trends in the MOC from surface forcing data alone. In addition, the lagged response of the MOC to the surface density fluxes may allow useful short-term (2–3 yr) forecasts of MOC variability to be made following further refinements of the method through analysis of alternative climate models and observational datasets. Such cost-effective forecasts would complement ensemble-based climate model forecasts that are now emerging.

Acknowledgments. The research of JPG and SAJ has been supported by a combination of the UK Natural Environment Research Council Oceans 2025 programme and Rapid Climate Change Grant NER/T/S/2002/00427. We thank Armin Köhl and Magdalena Balmaseda for providing their MOC time series. We acknowledge the British Atmospheric Data Centre for the supply of HadCM3 data, the NOAA Operational Model Archive and Distribution System (NOMADS) for the supply of the GFDL model data, and the WCRP CMIP3 multi-model database for the provision of BCM data.

REFERENCES

- Balmaseda, M. A., G. C. Smith, K. Haines, D. Anderson, T. N. Palmer, and A. Vidard, 2007: Historical reconstruction of the Atlantic Meridional Overturning Circulation from the ECMWF operational ocean reanalysis. *Geophys. Res. Lett.*, **34**, L23615, doi:10.1029/2007GL031645.
- Berry, D. I., and E. C. Kent, 2009: A new air–sea interaction gridded dataset from ICOADS with uncertainty estimates. *Bull. Amer. Meteor. Soc.*, **90**, 645–656.
- Bingham, R. J., C. W. Hughes, V. Roussenov, and R. G. Williams, 2007: Meridional coherence of the North Atlantic meridional

- overturning circulation. *Geophys. Res. Lett.*, **34**, L23606, doi:10.1029/2007GL031731.
- Boyer, T. P., S. Levitus, J. I. Antonov, R. A. Locarnini, and H. E. Garcia, 2005: Linear trends in salinity for the World Ocean 1955–1998. *Geophys. Res. Lett.*, **32**, L01604, doi:10.1029/2004GL021791.
- Bretherton, C. S., M. Widmann, V. P. Dymnikov, J. M. Wallace, and I. Bladé, 1999: The effective number of spatial degrees of freedom in a time-varying field. *J. Climate*, **12**, 1990–2009.
- Bryden, H. L., H. R. Longworth, and S. A. Cunningham, 2005: Slowing of the Atlantic meridional overturning circulation at 25°N. *Nature*, **438**, 655–657.
- Cunningham, S. A., and Coauthors, 2007: Temporal variability of the Atlantic meridional overturning circulation at 26.5°N. *Science*, **317**, 935–938.
- Curry, R. G., M. S. McCartney, and T. M. Joyce, 1998: Oceanic transport of subpolar climate signals to mid-depth subtropical waters. *Nature*, **391**, 575–577.
- Delworth, T. L., and Coauthors, 2006: GFDL's CM2 global coupled climate models. Part 1: Formulation and simulation characteristics. *J. Climate*, **19**, 643–674.
- Dickson, R. R., J. Meincke, S.-A. Malmberg, and A. J. Lee, 1988: The "Great Salinity Anomaly" in the northern North Atlantic 1968–1982. *Prog. Oceanogr.*, **20**, 103–151.
- , J. Lazier, J. Meincke, P. Rhines, and J. Swift, 1996: Long-term co-ordinated changes in the convective activity of the North Atlantic. *Prog. Oceanogr.*, **38**, 241–295.
- Eden, C., and J. Willebrand, 2001: Mechanism of interannual to decadal variability of the North Atlantic circulation. *J. Climate*, **14**, 2266–2280.
- Furevik, T., M. Bentsen, H. Drange, I. K. T. Kindem, N. G. Kvamstø, and A. Sorteberg, 2003: Description and evaluation of the Bergen climate model: ARPEGE coupled with MICOM. *Climate Dyn.*, **21**, 27–51.
- Gnanadesikan, A., and Coauthors, 2006: GFDL's CM2 global coupled climate models. Part II: The baseline ocean simulation. *J. Climate*, **19**, 675–697.
- Gordon, C., C. Cooper, C. A. Senior, H. Banks, J. M. Gregory, T. C. Johns, J. F. B. Mitchell, and R. A. Wood, 2000: The simulation of SST, sea ice extents and ocean heat transports in a version of the Hadley Centre coupled model without flux adjustments. *Climate Dyn.*, **16**, 147–168.
- Gregory, J. M., and Coauthors, 2005: A model intercomparison of changes in the Atlantic thermohaline circulation in response to increasing atmospheric CO₂ concentration. *Geophys. Res. Lett.*, **32**, L12703, doi:10.1029/2005GL023209.
- Grist, J. P., S. A. Josey, and B. Sinha, 2007: Impact on the ocean of extreme Greenland Sea heat loss in the HadCM3 coupled ocean–atmosphere model. *J. Geophys. Res.*, **112**, C04014, doi:10.1029/2006JC003629.
- , —, —, and A. T. Blaker, 2008: Response of the Denmark Strait overflow to Nordic Seas heat loss. *J. Geophys. Res.*, **113**, C09019, doi:10.1029/2007JC004625.
- Haine, T., and Coauthors, 2007: North Atlantic Deep Water transformation in the Labrador Sea, recirculation through the subpolar gyre, and discharge to the subtropics. *Arctic–Subarctic Ocean Fluxes: Defining the Role of the Northern Seas in Climate*, R. Dickson, J. Meincke, and P. Rhines, Eds., Springer, 653–701. [Available online at http://www.jhu.edu/~thaine1/Haine_etal07.pdf.]
- Johnson, H. L., and D. P. Marshall, 2002: A theory for the surface Atlantic response to thermohaline variability. *J. Phys. Oceanogr.*, **32**, 1121–1132.
- Josey, S. A., J. P. Grist, and R. Marsh, 2009: Estimates of meridional overturning from surface density flux fields. *J. Geophys. Res.*, in press.
- Kalnay, E., and Coauthors, 1996: The NCEP/NCAR 40-Year Reanalysis Project. *Bull. Amer. Meteor. Soc.*, **77**, 437–471.
- Knight, J. R., R. J. Allan, C. K. Folland, M. Vellinga, and M. E. Mann, 2005: A signature of persistent natural thermohaline circulation cycles in observed climate. *Geophys. Res. Lett.*, **32**, L20708, doi:10.1029/2005GL024233.
- Köhl, A., and D. Stammer, 2007: Variability of the meridional overturning in the North Atlantic from the 50 years GECCO state estimation. Rep. 43, Institut für Meereskunde, University of Hamburg, 38 pp.
- Kuhlbrodt, T., A. Griesel, M. Montoya, A. Levermann, M. Hofmann, and S. Rahmstorf, 2007: On the driving processes of the Atlantic meridional overturning circulation. *Rev. Geophys.*, **45**, RG2001, doi:10.1029/2004RG000166.
- Latif, M., C. Böning, J. Willebrand, A. Biastoch, J. Dengg, N. Keenlyside, and U. Schweckendiek, 2006: Is the thermohaline circulation changing? *J. Climate*, **19**, 4631–4637.
- Marsh, R., 2000: Recent variability of the North Atlantic thermohaline circulation inferred from surface heat and freshwater fluxes. *J. Climate*, **13**, 3239–3260.
- , A. J. G. Nurser, A. P. Megann, and A. L. New, 2000: Water mass transformation in the Southern Ocean of a global isopycnal coordinate GCM. *J. Phys. Oceanogr.*, **30**, 1013–1045.
- Nurser, A. J. G., R. Marsh, and R. G. Williams, 1999: Diagnosing water mass formation from air–sea fluxes and surface mixing. *J. Phys. Oceanogr.*, **29**, 1468–1487.
- Rhein, M., 1996: Convection in the Greenland Sea 1982–1993. *J. Geophys. Res.*, **101**, 18 183–18 192.
- Roberts, M. J., and R. A. Wood, 1997: Topography sensitivity studies with a Bryan–Cox-type ocean model. *J. Phys. Oceanogr.*, **27**, 823–836.
- Ronski, S., and G. Budéus, 2005: How to identify winter convection in the Greenland Sea from hydrographic summer data. *J. Geophys. Res.*, **110**, C11010, doi:10.1029/2003JC002156.
- Schmitt, F. W., P. S. Bogden, and C. E. Dorman, 1989: Evaporation minus precipitation and density fluxes for the North Atlantic. *J. Phys. Oceanogr.*, **19**, 1208–1221.
- Wolff, J., E. Maier-Reimerr, and S. Legutke, 1997: The Hamburg ocean primitive equation model. Tech. Rep. 13, Deutsches Klimarechenzentrum, Hamburg, Germany, 81 pp.
- Wunsch, C., 2005: The total meridional heat flux and its oceanic and atmospheric partition. *J. Climate*, **18**, 4374–4380.
- , and P. Heimbach, 2006: Estimated decadal changes in North Atlantic meridional overturning circulation and heat flux 1993–2004. *J. Phys. Oceanogr.*, **36**, 2012–2024.
- Yashayev, I., J. R. N. Lazier, and R. A. Clarke, 2003: Temperature and salinity in the central Labrador Sea during the 1990's and in the context of the longer-term change. *ICES J. Mar. Sci.*, **219**, 32–39.